THE DISTRIBUTION OF INORGANIC CATIONS DURING SPERMIOGENESIS IN THE MOUSE

A. L. KIERSZENBAUM, LAURA L. TRES, and C. J. TANDLER. From the Centro de Investigaciones sobre Reproducción, Facultad de Medicine, Buenos Aires, Argentina.

INTRODUCTION

Inorganic cations have been localized in several animal and plant tissues by means of the pyroantimonate fixation procedure (1–3). We demonstrated that an aqueous solution of potassium pyroantimonate enters the cell without disruption of cell membranes and produces electron-opaque cation-antimonate precipitates in a constant and reproducible manner.

The results obtained in mouse testis (3) were further extended to the meiotic prophase in spermatogenesis and to Sertoli's cells.[1] In the present paper we studied the distribution of pyroantimonate-precipitable cations during spermiogenesis. We demonstrate regional differences with respect to the occurrence of the precipitate of the spermatid during evolution.

MATERIALS AND METHODS

Adult Swiss mice (Rockland strain) were anesthetized with ether. The testes were fixed in a saturated solution of potassium pyroantimonate (Riedel–De Haën AG, Seelze, Hannover, Germany), pH about 9.2, hardened with formaldehyde, and postosmicated as described before (3).[1] The sections were examined unstained.

Staining of pyroantimonate-fixed sections was accomplished by first immersing the sections in a dilute solution of oxalic acid (1 vol of a saturated aqueous solution in 400 vol of distilled water), washing with distilled water, and then staining with uranyl acetate and lead citrate as usual.[1]

For conventional electron microscope fixation procedures, specimens were fixed in 2.5% glutaraldehyde in 0.1 M phosphate buffer pH 6.9 for 2 hr and postfixed in 1% buffered osmium tetroxide. Sections were stained with the usual uranyl acetate and lead citrate procedures.

Alcohol dehydration and embedding in Maraglas (Polysciences, Inc., Warrington, Pa.) were always employed. Sections were cut with glass knives on a Porter-Blum ultramicrotome and examined with a Siemens Elmiskop I electron microscope.

[1] L. L. Tres, A. L. Kierszenbaum, and C. J. Tandler. Submitted for publication.

RESULTS AND DISCUSSION

Spermatids fixed in potassium pyroantimonate exhibit patterns of cation-antimonate localization which are characteristic for the different phases of spermiogenesis. These changes involve the nucleus and the morphologic events occurring during spermatid maturation. Four major sites of precipitation have been shown. These sites are the spermatid–Sertoli's cell junction, the nucleus, the mitochondria, and the caudal portion of the head in mature spermatids.

During the whole spermiogenic process the area of contact between spermatids and Sertoli's cells is delimited by a heavy precipitate (Figs. 1, 3, and 5). This is particularly evident in the anterior part of spermatid head because the acrosome and the thin layer of Sertoli's cell cytoplasm disposed along the head of the mature spermatid are easily discernible (Fig. 5).

The inorganic cations at the contact of spermatids and Sertoli's cell are found accumulated mainly in the intercellular space and could be due to the permeability properties of plasma membranes. The same probably occurs at the membrane of the flagellum (Fig. 4). It could be asked whether an accumulation of anions, particularly inorganic phosphate (cf. reference 1, footnote 1), also occurs at those sites; if this is so, it would lower the solubility of divalent cations.

Within the spermatid, the acrosome and the cytoplasmic area between the acrosomal and plasma membranes are free of precipitate. In the contacting Sertoli's cell the dense fibrillar material disposed in parallel with the spermatid (4, 5) is also free of precipitate (Fig. 5). Inside the parallel cisternae of the Sertoli's cell, a few scattered antimonate precipitates are frequently encountered (Fig. 5). A discontinuous "layer" of antimonate deposit appears inside the mature spermatid at the posterior portion of the head. In the developing spermatid, when the cytoplasm has not yet shifted from the caudal pole of the nucleus (and the microtubules of the manchette appear) no antimonate deposit is evidenced at the caudal end. These observations strongly suggest that some event

takes place near the plasma membrane at the portions free of acrosomal material. A postacrosomal specialization of the inner aspect of the plasma membrane has been demonstrated (6). This corresponds to what was formerly called the postnuclear cap and is designated now as the postacrosomal dense lamina (6). This specialized structure (Figs. 5 and 6) must be the site of the inner discontinuous layer of antimonate precipitation; they occur at the same locations, i.e. they begin almost exactly at the posterior end of the acrosome, end abruptly at the junction of the lateral and caudal aspects of the nucleus, and do not continue over the back of the nucleus. Furthermore, they are absent in the developing spermatid when the manchette covers the caudal portion of the nucleus. The nuclear ring, i.e. the annular invagination of plasmalemma which marks the beginning of microtubules of the manchette, is free of antimonate precipitate. The finding of precipitation of cation-antimonate salts at the site of the postacrosomal dense lamina could explain the somewhat puzzling results obtained by Hall's microprobe analysis of mammalian sperm cells (7): a highly elevated zinc concentration (and probably other divalent cations, too) was found only near the junction of head and midpiece. In the light of the present finding, we suggest that the larger part of inorganic cations at the caudal pole is located in the extranuclear portion rather than within the posterior end of the nucleus itself. The physiological significance of an inorganic cation accumulation in the "postacrosomal cap" is not apparent at the moment, although the presence of a specialized structure at this site (6) certainly suggests some definite function (e.g., references 8, 9).

The most conspicuous changes in cation-antimonate distribution within the spermatid nuclei are related to changes in the condensation of chromatin. This in turn is related to the declining RNA-synthetic activity (10)[1] and, presumably, to the disappearance of ribonucleoprotein particles from these nuclei. Relatively abundant cation-antimonate precipitates are present in the spermatid at the earlier phases of spermiogenesis (Golgi and cap phases) (Fig. 1). The precipitate becomes scarcer as the acrosomal phase progresses and, finally, no sign of antimonate deposition is encountered in the elongated nuclei at the maturation phase (Figs. 4 and 5) when RNA synthesis is suppressed. The separation of nuclear envelope from the mass of condensed chromatin (Fig. 5) is a fixation artifact.

Figs. 1 and 2 show, respectively, a pyroantimonate-fixed immature spermatid at the Golgi phase and a similar spermatid after glutaraldehyde–osmium tetroxide fixation. The antimonate precipitates are not evenly distributed but occur in "patches;" this is also evident at the cap and acrosomal phases (cf. Fig. 1 in reference 4). Clusters of ribonucleoprotein particles are also distributed in "patches" (Fig. 2) and resemble, in size and distribution, the antimonate precipitate; these particles correspond apparently to the interchromatin granules described in several tissues (11).

The intramitochondrial antimonate deposit (Figs. 1 and 4) is a general phenomenon in pyroantimonate-fixed material, as it has been observed also in germinal cells during the male meiotic prophase and Sertoli's cells[1] as well as in other tissues (1, footnote 2, and in preparation). It has been suggested that the location of this type of precipitate—as seen after pyroantimonate fixation—probably coincides with the location of the "dense granules" observed after conventional-type fixations (1). However, this question requires further investigation.

SUMMARY

The localization of pyroantimonate-precipitable inorganic cations during spermiogenesis was

[2] A. L. Kierszenbaum, and C. J. Tandler. Submitted for publication.

FIGURE 1. Spermatid at the Golgi phase. Electron-opaque antimonate precipitates occur at spermatid–Sertoli's cell junction (arrows), in the Golgi complex (GC), in mitochondria (*mi*), and within the nucleus. *chr*, chromatin; *AV*, acrosomic vesicle; *AG*, acrosomic granule; *T*, tail. Pyroantimonate fixation. Stained with uranyl acetate and lead citrate. Scale mark, 1μ. × 16,000.

FIGURE 2. Spermatid at the Golgi phase fixed in glutaraldehyde–osmium tetroxide and stained with uranyl acetate and lead citrate. *chr*, chromatin; *ig*, interchromatin granules; *GC*, Golgi complex; *AV*, acrosomic vesicle. Scale mark, 1 μ. × 16,000.

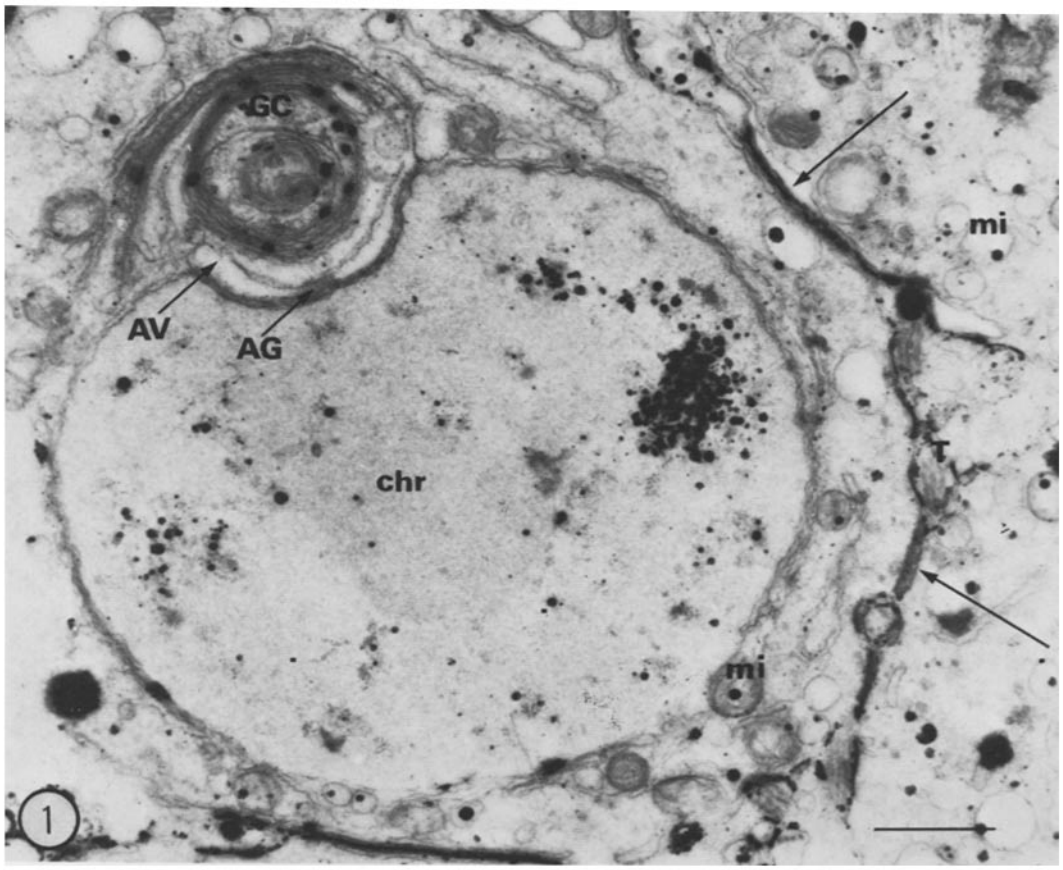
GC
AV
AG
chr
mi
mi
1

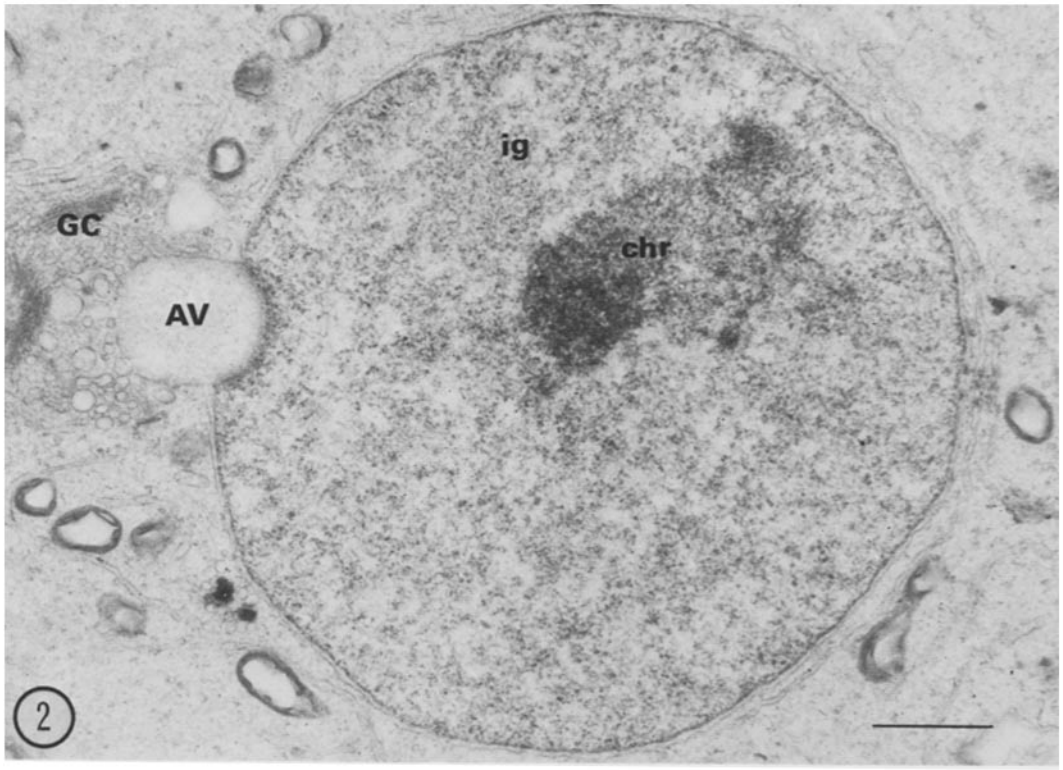
ig
GC
chr
AV
2

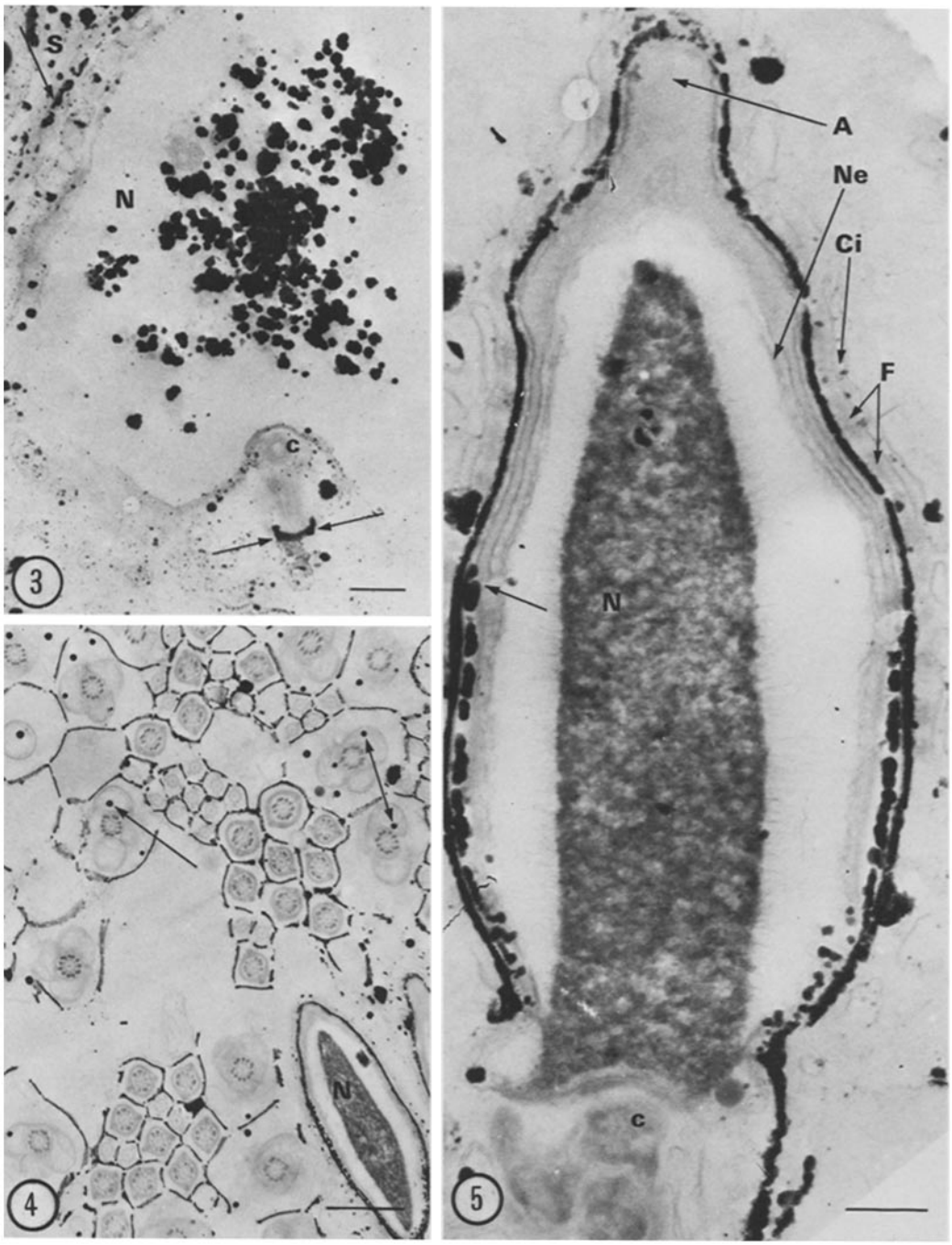

FIGURE 3. Developing spermatid showing cation-antimonate precipitates within the nucleus (*N*) and in the region of the annulus (between arrows). *c*, centriole; *S*, Sertoli's cell–spermatid junction (arrow). Pyroantimonate-fixation. Unstained. Scale mark, 0.5 μ. × 15,600.

FIGURE 4. Transverse section through spermatid tails at different levels; they are surrounded by antimonate precipitates at the junction with the Sertoli's cell. Antimonate deposits appear in mitochondria (arrows). *N*, nucleus of mature spermatid. Pyroantimonate fixation. Unstained. Scale mark, 1 μ. × 11,000.

FIGURE 5. Head of a mature spermatid, illustrating electron-opaque antimonate deposits in the intercellular space at the spermatid–Sertoli's cell junction. A second, discontinuous layer of precipitate appears at the caudal portion, beginning at the posterior end of acrosome (arrow). *A*, acrosome; *Ne*, nuclear envelope; *Ci*, parallel cisternae; *N*, nucleus. Pyroantimonate fixation. Unstained. Scale mark, 0.25 μ. × 47,700.

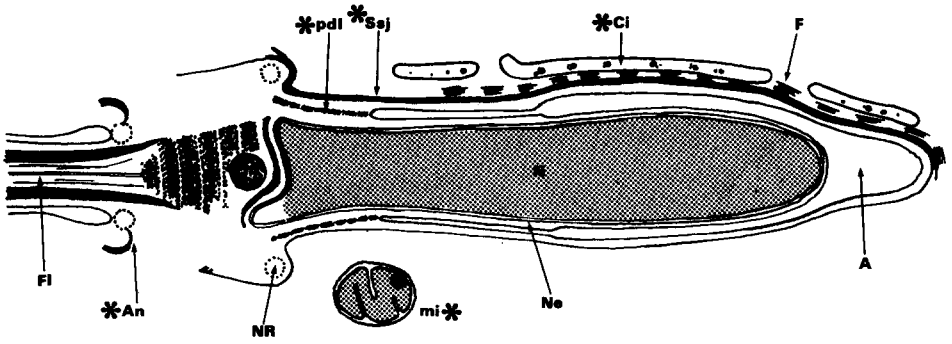

FIGURE 6. Summary diagram of mature spermatid head morphology and pyroantimonate localization. Thicker black lines indicate regions where pyroantimonate precipitate occurs; other precipitate is in the form of black dots. Postacrosomal dense lamina (*pdl*) is indicated at the posterior end of the acrosome (*A*) with a discontinuous black line. Abbreviations (* indicate regions of pyroantimonate-precipitable inorganic cations): *Ssj*, Sertoli's cell–spermatid junction; *Ci*, parallel cisternae; *An*, annulus; *mi*, mitochondria; *N*, nucleus; *Ne*, nuclear envelope; *NR*, nuclear ring; *Fl*, flagellum; *F*, fibrils.

studied in mouse testis fixed in potassium pyroantimonate, hardened with formaldehyde, and postosmicated. The main sites of cation accumulation are: (*a*) in the intercellular space at the spermatid–Sertoli's cell junction; (*b*) at the membrane of the flagellum in developing spermatids; (*c*) in the caudal portion of the head in mature spermatids, beginning at the posterior end of the acrosome and located most probably in the postacrosomal dense lamina; (*d*) in the nucleus of immature spermatids, probably in the area of interchromatin granules; and (*e*) within mitochondria.

The authors wish to express their thanks to Professor R. E. Mancini for providing the facilities for this study. We gratefully acknowledge the outstanding assistance of Miss Estela L. Kirlis.

This investigation was supported by a grant from the Consejo Nacional de Investigaciones Científicas y Técnicas, Argentina and The Population Council, Inc., New York. Drs. Tres and Tandler are established investigators of the C.N.I.C.T.

Received for publication 28 September 1971, and in revised form 8 November 1971.

REFERENCES

1. TANDLER, C. J., and A. L. KIERSZENBAUM. 1971. *J. Cell Biol.* **50**:830.
2. TANDLER, C. J., C. M. LIBANATI, and C. A. SANCHIS. 1970. *J. Cell Biol.* **45**:355.
3. KIERSZENBAUM, A. L., C. M. LIBANATI, and C. J. TANDLER. 1971. *J. Cell Biol.* **48**:314.
4. FLICKINGER, C. J. 1967. *Z. Zellforsch. Mikrosk. Anat.* **78**:92.
5. BURGOS, M. H., R. VITALE-CALPE, and A. AOKI. 1970. *In* The Testis. A. D. Johnson, W. R. Gomes, and N. L. Vandemark, editors. Academic Press Inc., New York. **1**:551.
6. FAWCETT, D. W. 1970. *Biol. Reprod.* **2**:90.
7. HALL, T. A. 1966. *In* X-Ray Optics and Microanalysis. Casting, Descamps, and Philibert, editors. Hermann, Paris. 679.
8. DARZYNKIEWICS, Z., B. L. GLEDHILL, and N. R. RINGERTZ. 1969. *Exp. Cell Res.* **58**:435.
9. BRACKETT, B. G., W. BARANSKA, W. SAWICKI, and H. KOPROWSKI. 1971. *Proc. Nat. Acad. Sci. U. S. A.* **68**:353.
10. MONESI, V. 1965. *Exp. Cell Res.* **39**:197.
11. MONNERON, A., and W. BERNHARD. 1969. *J. Ultrastruct. Res.* **27**:266.